Advancements in Zinc-Air Redox Flow Batteries: Investigating the Role of Carbopol® Microgel Adsorption on Zinc microparticles

Diego Milián, Yahya Rharbi, Nadia El Kissi

Advancements in Zinc-Air Redox Flow Batteries: Investigating the Role of Carbopol® Microgel Adsorption on Zinc microparticles

Diego Milian, Yahya Rharbi, Nadia El Kissi[1]

Univ. Grenoble Alpes, CNRS, Grenoble INP, LRP, 38000 Grenoble, France

Keywords: Zinc-Air Redox Flow Batteries, Carbopol® Microgel, Adsorption, Microparticle Sedimentation, Rheology Analysis, UV-Vis Spectroscopy, Stabilization Strategies

Abstract

This research investigates zinc slurry–air redox flow batteries (Zn-air RFBs) as a means for energy storage, specifically addressing the challenge of zinc microparticle sedimentation in alkaline battery environments. The study explores the potential of yield stress fluids, particularly PAA (Carbopol®) microgels, as stabilizers for zinc particles during battery operation, and regarding sedimentation in particular. Two effects that can limit the effectiveness of PAA yield stress in stabilizing the suspension are examined in this study. First is the ionic strength and pH that can evolve during the slurry formulation. The second effect is associated to zinc polymer interactions that can develop during the suspension preparation. Using methodologies such as reverse rheology and UV-Vis spectroscopy, the research identifies that the primary stabilization challenge is the adsorption of Carbopol® microgels onto zinc surfaces, which significantly influences the gel's yield stress. These insights contribute to an enhanced understanding of the physical chemistry of the suspending fluid, facilitating the development of more efficient and stable Zn-Air RFBs.

1. Introduction

The current energy policies strongly emphasize the reduction of greenhouse gas emissions, prioritizing renewable energy sources as the primary means of providing electricity to large communities (European Commission in 2019). However, renewable sources, such as solar and

[1] Corresponding author: *nadia.elkissi@univ-grenoble-alpes.fr;*

wind, face significant challenges due to their intermittent nature, highlighting the need for efficient energy storage solutions.

Among various promising energy storage solutions, redox flow batteries (RFBs) have garnered significant attention due to their design flexibility, cost-effectiveness, safety features, and the capability to separate power output from energy capacity. This separation allows for the customization of the design to meet specific market requirements.

Recently, a different design was proposed to undertake the problem of low solubility compounds affecting battery energy density.(Choi et al. 2020) This design consists in a semi-solid flow cell, in which the electro active materials are suspended in electrolyte media producing a slurry with higher energy density than its aqueous analogue.(Duduta et al. 2011) This approach has been applied to several metal-air batteries, chiefly high energy density zinc-air batteries, reducing anode limitations, like zinc passivation, corrosion and dendrite formation.(Fu et al. 2017; Han et al. 2018)

The zinc slurry–air RFB, the focus of this study, consists mainly in a zinc slurry electrolyte anode, a membrane, and an air cathode (Choi et al. 2020). However, one of the primary challenges for this technology lies in mastering the organization of zinc particles within the suspending fluid to effectively control electrical transfer. In that sense, the percolation and porosity of the network formed by the zinc microparticles within the suspending fluid play a crucial role, highlighting the significance of the suspending fluid for the overall process (Zhu et al. 2020).

Furthermore, it is imperative to give thorough attention to the physical chemistry properties of the suspending fluid, especially because zinc-air batteries usually operate in concentrated alkaline KOH electrolyte environment (Visco et al. 2014; Mainar et al. 2018). Therefore, one of the primary challenges faced by zinc-air RFBs is the selection of the right suspending fluid and the formulation of a gelling medium able to disperse dense zinc microparticles uniformly, prevent their sedimentation and regulate their percolation, within the harsh alkaline battery environment.

Retarding or inhibiting sedimentation of dense microparticles is commonly achieved by using a suspending fluid with high viscosity or a yield stress fluid. Given that yield stress fluids resist flow below a stress threshold (yield stress), acting as a semi-solid state below and flowing above it, they prove especially effective in preventing settling of particles in suspensions. More generally, the use of yield stress gels to prevent sedimentation is a subject of considerable

interest with numerous industrial applications (Emady et al. 2013). This is achieved by raising the yield stress value of the gel above the stress applied by the stabilized particles. Sedimentation is anticipated within a confined yield region surrounding the particle, influenced by gravitational forces or external shear stresses (Singh et al. 1991; Wünsch 1994; Ferroir et al. 2004; Tabuteau et al. 2007; Merkak et al. 2009; Ovarlez et al. 2012).To quantify sedimentation, a dimensionless yield stress is used, defined as the ratio of the fluid yield stress (τ_y) to the stress exerted on the fluid by particles with a radius (R) and density (ρ_p):

$$Y = \frac{1.5\,\tau_y}{g.R.(\rho_p - \rho_f)} \quad (1)$$

Here, ρ_f represents the fluid density, and g represents gravitational acceleration(Beris et al. 1985). Sedimentation analysis is typically quantified using a critical Y value, known as Ycrit, below which sedimentation occurs.

Carbomers are suggested as good candidates for this purpose. They consist in crosslinked polyacrylic acid (PAA), mostly known by its commercial name Carbopol®. We will refer to this carbomer as PAA or Carbopol® hereafter. PAA gels are spongy crosslinked microgels that are defined as colloidal glasses (Emady et al. 2013), in which the yield stress is a macroscopic property of the jammed repulsive interactions in its microstructure (Sollich et al. 1997; Coussot et al. 2002). This polymer is widely used as a model yield stress fluid with easily adjustable yield stress levels, achieved through changes in gel concentration, degree of ionization, or ionic strength.

As the pH of the solution approaches the pKa value of Carbopol®, around 6, the acrylic acid groups begin to ionize (Lee et al. 2011). This ionization leads to electrostatic repulsion between the chains, initiating the swelling of PAA microgels in water (Lee et al. 2011; Lefrançois et al. 2015). The swelling process subsequently triggers jamming, eventually resulting in a yield stress behavior, (Oppong and de Bruyn 2011). Increasing the pH far beyond the pKa or introducing salts screens the electrostatic repulsion between acrylic acid groups, leading to polymer chain contraction, reduced swelling, and consequently, decreased yield strength and viscosity (Jaworski et al. 2022).

PAA has been routinely used to suspend zinc microparticles in RFBs and its crucial role in the suspending performance in the battery formulation was underlined (Wu et al. 2006; Faegh et al. 2018; Zhu et al. 2020; Tran et al. 2020).

Regarding sedimentation inhibition, numerous studies on PAA have emphasized sedimentation occurring below a critical yield value (Ycrit), ranging from 0.14 to 0.39 (Beris et al. 1985; Atapattu et al. 1995; Merkak et al. 2006; Emady et al. 2013). However, these investigations often overlook the chemical interactions between particles and the suspending gel while assuming low particle concentration. These two considerations may not be directly applicable to zinc-air RFBs applications, where charged zinc particles are present at high concentrations, with the potential for strong interactions with PAA. For example, a sedimentation study involving 30 wt% zinc particles in PAA and Attapulgite has shown behavior that falls outside this Ycrit range (Milian et al. 2023).

Moreover, the ionic strength sensitivity of PAA becomes particularly critical in the presence of zinc particles or when exposed to the harsh alkaline conditions encountered during battery usage (Visco et al. 2014; Mainar et al. 2018). In fact, according to zinc Pourbaix diagram, zinc releases various ions depending on the pH conditions (Zhang 1996): Zn^{2+} in the acidic to neutral region, zinc oxide (ZnO) and zinc hydroxide ($Zn(OH)_2$ up to pH = 11, and $Zn(OH)_3^-$. and $Zn(OH)_4^{-2}$ at higher pH. Thus, it is important to understand how the released ions affect the swelling ratio of PAA near the zinc particles and in the bulk and how this modifies the jamming mechanism, yield stress, and viscosity; properties that are all crucial in controlling the stability of the suspension.

Finally, investigations into complex suspensions featuring particles that have the potential to interact with PAA, such as bentonite, magnetite ferrite, or $CaCO_3$, particularly emphasize the adsorption of PAA microgel onto suspended particles (Viota et al. 2005; Li et al. 2010; Kelessidis et al. 2011). Thus, the attractive interactions between the positively charged zinc and the negatively charged acrylic acid are likely to induce adsorption and complexation mechanisms that could affect the jamming of the microparticles, thus modifying the suspending ability of PAA. Therefore, it is important to assess the relevance of complexation and adsorption mechanisms in the formulation of the zinc particles suspension.

The aforementioned findings highlight the importance of the interplay between PAA microgel and zinc microparticles in governing the gel's yield stress and its ability to suspend zinc particles and avoid sedimentation. Consequently, for the effective formulation of suspending gels, particularly in case of zinc slurry for RFBs application, it is crucial to understand first, how the adsorption of PAA onto zinc particles affects gel yield stress and sedimentation. (Curran et al. 2002; Nelson and Ewoldt 2017). How the released zinc ions affect PAA's

swelling ratio near the zinc particles and in the bulk, and how this change influences yield stress, is the second question to be answered.

This study focuses on understanding the interactions between PAA and zinc particles and their role in stabilizing zinc within the context of a zinc-air RFB application, i.e. a high particle concentration and a strong alkaline environment.

The effect of zinc sedimentation will be first presented and discussed.

Then, to study zinc/polymer interactions, the approach consists first in investigating the adsorption of Carbopol® microgel onto zinc particles and its impact on the yield stress and the suspending performance of the slurry. This will be done first through analysis of the rheological behavior of supernatants recovered from the centrifugation of a zinc suspension in a PAA gel. Supernatants will allow to evaluate the remaining PAA concentration in the supernatant that will be compared to that of the original gel. Additionally, UV-Vis spectroscopy, combined with rhodamine dye labeling, is employed to validate the adsorption process.

Finally, the effects of zinc ionization on PAA yield stress and the impact of PAA swelling in the vicinity of zinc particles during the adsorption process will be investigated.

2. Materials and Methods

2.1 Material.

Carbopol® 940 (Acros Organics), a crosslinked polyacrylic acid powder, referred hereafter as PAA or Carbopol®, was used in its as-received state without the need for further purification.

Zinc particles (zinc powder battery grade, GN 7-4/200Bi/200In, Grillo GmbH) were employed as received. The size distribution of these particles was determined via laser diffraction granulometry using a Mastersizer 2000 from Malvern analytical. The results indicated a Gaussian disperse distribution ranging from 30 µm to 120 µm, with an average size of 76.4 µm (Milian et al. 2023).

PAA solutions and zinc suspensions were prepared using doubly deionized water.

Sodium hydroxide (NaOH) from Sigma Aldrich was employed for pH adjustment when necessary. pH measurements were conducted using an Orion Star A215 pH/Conductivity meter from Thermo Fisher Scientific, along with a pH/ATC rechargeable electrode (Orion™ ROSS Ultra™ Triode™).

Rhodamine 6G from Sigma Aldrich was used for labeling the PAA solution.

2.2 PAA solutions preparation

A stock solution of 0.30 wt. % crosslinked polyacrylic acid (PAA) gels was prepared as follows: The Carbopol® polymer was slowly added to deionized water under continuous agitation using a magnetic stirrer set at 800 rpm. The mixture was left under stirring for 24 hours to ensure complete homogenization and hydration (R. Varges et al. 2019). The resulting solution had a pH of 3.6.

Gels with concentrations ranging from 0.10 to 0.30 wt. % were prepared by diluting the stock solution with deionized water and stirring with a magnetic stirrer at 800 rpm for 2 hours. The pH of each gel was adjusted to various values within the range of 4 to 14 by gradually adding 1M NaOH solution while stirring with a vacuum paddle-mixer (Vacuret-S, Reitel GmbH) under a vacuum pressure of -0.8 bar. After their preparation, the samples were stored at ambient temperature for 24 hours before use. In cases where a higher pH above 11 was required, a 5M NaOH solution was used to adjust the pH without altering the concentration.

2.3 Zinc suspensions and supernatant preparation for adsorption measurements

To prepare zinc suspensions that will be later centrifuged to obtain the supernatant for adsorption measurements, only PAA gels at pH 7 were studied. To do so, PAA gels were individually placed in 25 mL centrifuge tubes. Next, for each PAA gel concentration considered, zinc particles are added in the tubes and mixed using a vortex shaker (Vortex-Genie® 2, Scientific Industries), until a homogeneous blend was visually confirmed. The concentration of zinc particles in the gel solution was maintained within the range of 0 to 60 wt%.

As zinc suspensions are not neutral-buoyant systems (i.e. particle density equal to suspending fluid density), they can undergo sedimentation (Ovarlez et al. 2015). The effect of PAA on zinc sedimentation is presented in section 3.1 below. To avoid this phenomenon the PAA-zinc suspensions were subjected to continuous agitation at 10 rpm using a rotating mixer (RM5, Assistant®, Hecht Glaswarenfabrik GmbH & Co KG) for a duration of 24 hours. Subsequently, the samples underwent centrifugation at 500 rpm for 10 minutes, and the resulting supernatant was meticulously extracted and subjected to analysis. This analysis included pH measurement, rheological testing, and, in the case of dye-labeled PAA gel (see below), UV absorption measurements.

Supernatants recovered after centrifugation are free from zinc thus indicating that the sample corresponds only to PAA gel (see supplementary material S1). They will be addressed as S_{p_zn}[2], where ''p'' is the PAA concentration and ''zn'' the fraction of zinc in the parent suspension in wt. %. The liquid remaining after sedimentation, now referred to as the suspending gel (SG) for simplicity, is thus essentially a polyacrylic acid (PAA) solution. This solution comprises the portion of unbound PAA that did not settle with zinc during the sedimentation process and is indicative of the suspending medium.

2.4. Labelling and UV-Vis spectroscopy

Polyacrylic acid (PAA) was labeled with rhodamine 6G (R6G) from Sigma Aldrich through the complexation of COO- groups with the cationic groups of R6G (Beija et al. 2009; Haack et al. 2017; Dinkgreve et al. 2018). To accomplish this, 0.5 wt % of PAA at pH 7 was mixed with a dye solution of 10^{-5} M at a volume ratio of 1:4. The mixture was then stirred in a paddle mixer for 1 hour.

To assess the efficiency of rhodamine labeling of Carbopol®, the labeled Carbopol® was separated from the aqueous phase by precipitation using branched polyethyleneimine (Sigma Aldrich, Mw 25 kg/mol). For this, a polyethyleneimine solution was added to the labeled Carbopol® solution while stirring for one hour. The aqueous phase was then separated from the solid polymer through filtration. The clarity of the resulting filtrate indicated that most of the rhodamine dye was bound to the PAA polymer.

[2] Sp_0, corresponds to the PAA gel that was used to prepare the corresponding zinc suspensions and its associated supernatants

The concentration of rhodamine in the R6G labelled Carbopol® solution (PAA_R6G) was determined by measuring the UV absorption using a UV-Vis spectrometer (Red Tide USB650 Fiber Optic Spectrometer, Ocean Insight) equipped with a 1 cm path length cell. The absorption was quantified at the maximum absorption peak of R6G, with a wavelength λ = 525 nm. To ensure the validity of Beer-Lambert's law ($A = \epsilon \cdot l \cdot c$) [3], absorbance readings were kept below 2. In instances where absorption exceeded 2, the solution was diluted with water. The extinction coefficient ϵ of R6G in aqueous PAA_R6G solution was assumed to be similar to that of free R6G in water. The PAA_R6G concentrations were thus estimated using the R6G ϵ value. The extinction coefficient ϵ was estimated by preparing several aqueous solutions of R6G at different concentrations, and ϵ was calculated from the slope of the linear relationship between absorbance A vs. dye concentration to be around 92,000 cm^{-1} M^{-1}.

The quantification of Carbopol®'s absorption on zinc particles was conducted using fluorescence techniques with dye-labeled Carbopol® (PAA_R6G) at a concentration of 0.10 wt. %. The PAA_R6G was mixed with a zinc suspension at concentrations ranging from 0 to 20 wt %. Mixing was carried out using vortex shaker (Vortex-Genie® 2, Scientific Industries) as described above. Afterwards, the PAA_R6G was separated from the zinc through centrifugation. The obtained supernatant was analysed using UV spectroscopy to quantify the PAA_R6G concentration, utilizing Beer-Lambert's law and the ϵ value.

2.5. Rheological measurements

Rheological characterization was performed at 20 °C using a stress-controlled rheometer DHR-3 (TA-instruments) equipped with a cone-plate geometry. The cone had a radius of 25 mm and an angle of 2 degrees. Both cone and plate had rough surfaces to avoid sample slippage (Coussot 2005). The experiment was protected from potential solvent evaporation by using a solvent trap. Steady state measurements were performed by applying constant shear rate steps. Measurements were performed two times by increasing and decreasing shear rate steps to check reproducibility. Lastly, steady state flow curves were fitted to Herschel-Bulkley model (Equation 2) to determine rheological flow parameters, chiefly yield stress τ_y.

[3] With A the absorption, ϵ the extinction coefficient, l the length cell and c the dye molar concentration.

$$\tau = \tau_y + K\dot{\gamma}^n \quad (2)$$

When viscosity of the sample was found to be too small to be characterized by a cone-plate geometry, a microviscometer (Lovis 2000 microviscometer, Anton Paar), based on the rolling ball principle was used (Hubbard and Brown 1943).

3. Results and discussions

3.1. Stabilization vs. sedimentation of zinc in the context of zinc-air RFBs application: i.e. high zinc concentration and alkaline environment

The results obtained in this section are deduced from the work by Milian et al., 2023. In that study, the sedimentation of micron-sized zinc particles at 30 wt% in concentration, was examined using a model suspending gel based on a PAA/attapulgite mixture in alkaline condition (10M KOH). In that study, the gel's yield stress was adjusted by varying the concentration of PAA between 0.2 wt % and 0.6 wt%, the attapulgite being fixed at 0.9 wt %. The progression of the sedimentation front was monitored at different intervals during the sedimentation process using a camera. The yield stress of the gel was independently measured using rheometry, employing the Herschel-Bulkley fit method for analysis. The average sedimentation velocity was determined and plotted against the calculated dimensionless yield stress Y for the different gel compositions, which is derived from the fluid yield stress τ_y using equation 1. Figure 1 illustrates the decrease in sedimentation velocity as Y increases, underscoring the critical role of yield stress in preventing sedimentation. As Y increases, the estimated sedimentation velocity decreases, ultimately approaching a value near zero at the critical yield stress Y_{crit}, signifying the onset of efficient stabilization. Notably, for the suspending gel considered in the study by Milian et. al, 2023, the recovered Y_{crit} is approximately 1. As indicated in section 1, this Ycrit is three times higher than values of 0.14 to 0.39 reported in previous studies involving PAA with metal or plastic particles (Beris et al. 1985; Atapattu et al. 1995; Merkak et al. 2006; Emady et al. 2013).

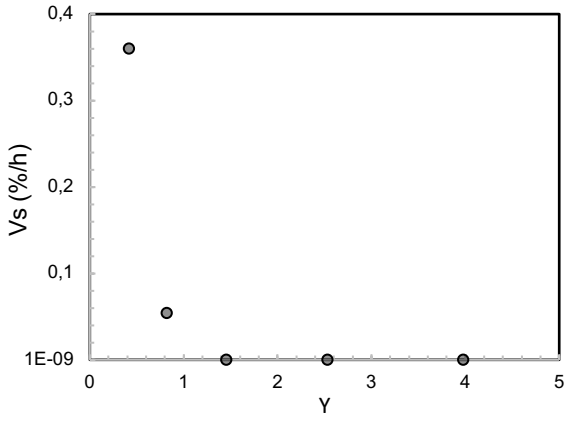

Figure 1. Apparent sedimentation velocity of zinc particles in gels composed of PAA and attapulgite. PAA concentration was varied between 0.2 wt % and 0.6 wt %. Attapulgite and zinc concentration were maintained at 0.9 wt % and 33.8 wt% respectively. The measurements are determined from results in Milian et al, 2023. These velocities are plotted against the dimensionless yield stress Y, which is derived from the fluid yield stress τ_y using Equation 1.

The discrepancy in Y_{crit} in comparison to the existing literature on PAA could potentially be clarified by two main distinctions. Firstly, the suspended particles exhibit rich ionic properties, as demonstrated by the Pourbaix diagram (Zhang 1996), leading to alterations in both pH and ionic strength. The second notable difference lies in the zinc concentration, exceeding 33.8wt% in Milian et al.(Milian et al. 2023), as opposed to the lower concentrations investigated in prior studies (Beris et al. 1985; Atapattu et al. 1995; Merkak et al. 2006; Emady et al. 2013). These variations raise questions about how zinc/PAA interactions or the presence of ionic species might impact the gel's yield stress and, consequently, the sedimentation process.

Addressing these issues involves initially investigating the influence of pH on the yield stress of the PAA solution. Subsequently, experiments were conducted to examine the interactions between zinc and PAA and their impact on the gel's yield stress. As outlined in section 1, this examination will employ both an indirect approach using rheometry and direct measurements based on UV-Vis spectroscopy.

3.2. Effect of pH on the yield stress of PAA solutions

Flow behavior of PAA gel 0.10 wt. % at different pH is displayed in figure 2a. The shear stress response to a shear rate is shown to depend strongly on pH. Two main behaviors can be observed from the data set in the pH range studied. For the lowest and highest pH, being 4 and 14 respectively, a viscoelastic behavior is observed. Conversely, for gels at pH from 6 to 12 a viscoplastic behavior is observed, evidenced by the yield stress at low shear rates followed by

shear thinning behavior when the shear rate increases. In addition, it is observed that at a given shear rate, shear stress values increase with increasing pH up to a pH of 7, where shear stresses found a maximum value. As pH is further increased, shear stresses values decrease. These findings align with literature on similar PAA materials (Piau 2007; Lee et al. 2011; Oppong and de Bruyn 2011; Gutowski et al. 2012; Lefrançois et al. 2015; Jaworski et al. 2022): at a pH around the pKa, being 6 for Carbopol®, (Lee et al. 2011) the shear stress of fully ionized PAA exhibits a yield stress behaviour; for pH beyond and below the pKa PAA chains are not fully extended (are contracted), the swelling ratio is lower, and jamming is less pronounced.

The same experiments were performed on PAA gels concentrations between 0.15 and 0.30 wt. %. For gels showing a viscoplastic behavior, yield stress values were determined by fitting the flow curves to Herschel-Bulkley model (equation 2). The resulting yield stress is represented as function of pH for different concentrations in figure 2b. In this figure, a value of zero was assigned to the yield stress for samples with a viscoelastic behavior.

It is thus clearly shown that across all tested concentrations of PAA, ranging from 0.10 to 0.30 wt. %, there is an initial increase in yield stress as the pH rises, reaching a peak at a pH of 6-7, close to Carbopol®'s pKa of 6. This is followed by a decrease in yield stress as the pH continues to increase. This trend aligns with existing research, highlighting that the ionization state of PAA chains at various pH levels is a key determinant of their rheological behavior (Piau 2007; Lee et al. 2011; Gutowski et al. 2012; Jaworski et al. 2022).

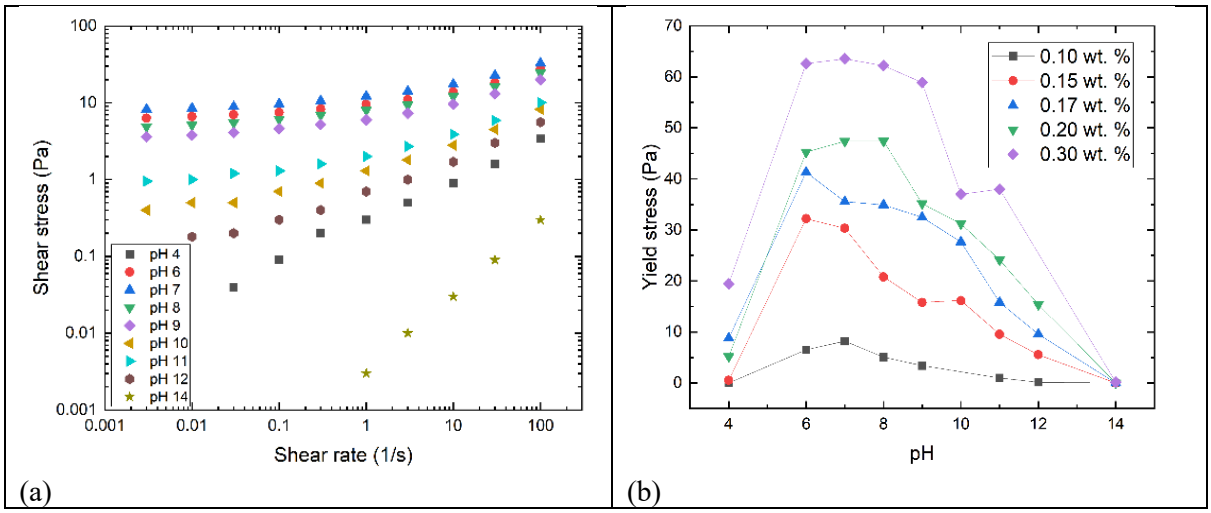

Figure 2. a) Shear stress as function of shear rate for PAA gel 0.10 wt. % at different pH. b) Yield stress τ_y obtained from Herschel-Bulkley model, as function of pH for different PAA concentrations.

3.3. Impact of zinc on the physical chemistry and rheological characteristics of suspending gels

The ability of a PAA gel to suspend dense zinc particles was found to be dependent on the zinc fraction. Specifically, at low zinc fractions (< 10 wt%), zinc remains suspended within the PAA gel at a concentration of 0.1wt % and 0.15 wt%. However, at higher zinc fractions, particularly at 40 wt% and 60 wt%, the zinc particles precipitate, leading to a supernatant gel ranging from clear to turbid. This observation underscores that sedimentation is influenced not only by the yield stress of the PAA gel but also by the zinc content in the mixture. Potential reasons for this behavior may include the impact of zinc on the physical properties, pH for example, and rheological characteristics of the PAA gel. Additionally, the concentration of the gel might decrease due to adsorption onto zinc particles.

3.3.1 Effect of zinc on the pH of the suspending gel

After mixing zinc with the PAA gel and agitating the mixture for 24 hours, a noticeable increase in pH was observed, significantly surpassing the pH of the initially prepared PAA gels without zinc (S_{p_0}). It is noteworthy that the initial PAA gels (S_{p_0}) had a pH of 7 at the time of suspension preparation. As indicated in §2.3., the prepared suspension then underwent centrifugation, resulting in the separation of the suspending gel (SG) in the supernatant from the zinc in the infranatant. The pH of the SG was then measured, and the results are presented in figure 3. It is observed that the SG's pH increased significantly, transitioning from its initial pH of 7 in the absence of zinc, to a range between 10.5 and 11 at zinc concentration around 10wt% and remains almost constant beyond. Notably, this trend was consistent across all the PAA concentrations investigated in this study.

The notable changes in the physicochemical properties of the PAA gel upon mixing with zinc are expected due to zinc's electrochemical behaviour (Guo and He, 2023; Konarov et al., 2018; Zhang, 1996). Indeed, zinc is selected for battery applications owing to its redox activity, with a redox potential of -0.76 V (Guo and He, 2023). As summarized in the Zn Pourbaix diagram, when in water, solid zinc initiates an oxidation process, leading to the generation of soluble Zn^{2+} ions. Following this, the Zn^{2+} ions engage in a reaction to form soluble $Zn(OH)^{+}$ and zinc hydroxide, $Zn(OH)_2$, which exhibits reduced solubility. This compound can then participate in additional reactions, yielding a variety of soluble zinc ions, notably $Zn(OH)_4^{2-}$ and $Zn(OH)_3^{-}$. (Parsons 1964; Konarov et al. 2018; McMahon et al. 2019). According to various studies, such as the one by McMahon et al.(McMahon et al. 2019), redox reactions predominantly produce

soluble Zn^{2+} ions in acidic conditions (with a pH below 4). As the pH increases, these ions transform into zinc hydroxide ($Zn(OH)_2$) and zinc oxide (ZnO). In slightly alkaline conditions (pH between 8.0 and 10), $Zn(OH)_2$ and ZnO emerge as the more prevalent species. When the pH exceeds 11, $Zn(OH)_2$ converts into zincate ions, predominantly $Zn(OH)_4^{2-}$.

To further explore the effect of soluble ionic species on the PAA gel, it's important to evaluate their concentrations, especially those of Zn^{2+} and $Zn(OH)_4^{2-}$. The equilibrium pH observed in this experiment, ranging between 10.4 and 11, falls within the predicted pH range where insoluble $Zn(OH)_2$ is at its maximum, and the combined concentrations of soluble ions Zn^{2+} and $Zn(OH)_4^{2-}$ is at its minimum. According to (McMahon et al., 2019), the ion concentrations vary with pH as follows: $[Zn^{2+}] = 10^{(-12.58-2pH)}$ and $[Zn(OH)_4^{2-}] = 10^{(-30.24+2pH)}$. Utilizing these estimations, the pH at which the concentrations of $[Zn^{2+}]$ and $[Zn(OH)_4^{2-}]$ are balanced and their sum is minimized is estimated to be around 10.7. This closely aligns with the measured equilibrium pH from this experiment (10.4 – 11). At this pH level, the concentrations of both $[Zn^{2+}]$ and $[Zn(OH)_4^{2-}]$ equal 1.5×10^{-9} mol/L.

This result clearly shows that the redox activity of Zn in water is one of the most important factors in defining the physicochemical properties of the SG, which in turn affects its rheological properties and consequently its suspending aptitude. The pH of the SG is mostly defined by the equilibrium between the released species during the zinc redox reaction, namely Zn^{2+}, $Zn(OH)_4^{2-}$, and $Zn(OH)_2$, and therefore controls the ionization degree of the SG. Indeed, the optimal ionization of most acrylic acids in Carbopol® occurs at a pH close to its pKa, around 6 (Lee et al. 2011), thus maximizing yield stress at pH levels around 6 - 8, as illustrated in Figure 2b. However, increasing the pH beyond the pKa, to between 10 and 11 and liberating soluble ionic species (Zn^{2+}, $Zn(OH)_4^{2-}$), through zinc redox reactions generates additional ionic strength, leading to the screening of electrostatic repulsion between PAA chains. This causes chain shrinking and a consequent decrease in yield stress, as also depicted in Figure 2b.

This indicates that one should not rely on the intrinsic rheological properties of the SG for predicting the Zn stabilization process. Instead, attention should be given to the properties that align with the redox equilibrium condition at specific pH values, which, in this case, are between 10 and 11. Indeed, as illustrated in Figure 2b, it is noteworthy that the PAA yield stress (τ_y) decreases by 40 to 50% as the pH deviates from its initial value of 7 to the redox equilibrium value around 10 to 11.

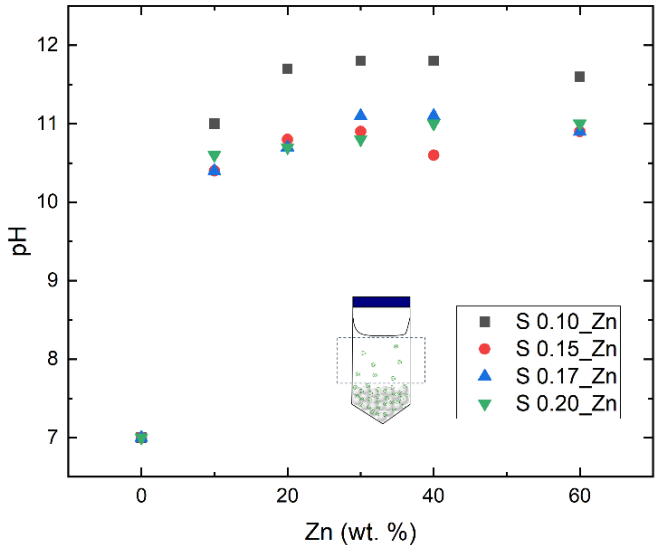

Figure 3. pH variation of SG as a function of Zn weight fraction in parent Zn suspensions. The SG is prepared by mixing PAA at various concentrations (0.1, 0.15, 0.17, and 0.2 wt%) with zinc at different fractions, under agitation, followed by separation through centrifugation. The supernatant, designated as the SG, is then subjected to pH measurement. The legend (S_{p_zn}) denotes sample specificity, where "p" represents the fraction of the initial PAA concentration.

3.3.2. Effect of zinc on the flow behavior and yield stress of the suspending gel

The suspending gel (SG), which refers to the supernatant obtained after separating the PAA gel from Zn following mixing, is further analyzed using steady shear rheometry across various shear rates. Figure 4 is a typical graph depicting shear stress vs. shear rate relationships for a series SG compositions prepared by mixing one PAA gel fraction 0.15 wt% with various zinc fractions between 0 and 60 wt% ($S_{0.15\_zn}$). The SG in the absence of Zn ($S_{0.15\_0}$ in black squares) shows, as expected, all the characteristics behaviors of an ionized PAA gel, with a yield stress at low shear rates, followed by shear thinning at higher shear rates. With an increase in zinc concentration, the overall shear stress decreased, which indicates a reduction in viscosity. Shear thinning behavior of SG was observed for all zinc fractions used in this experiment. The rheological behaviors are consistent across all examined PAA concentrations, from 0.1 wt.% to 0.2 wt% and for all zinc fractions from 0 up to 60 wt.% (figure 5).

Flow curves of SG in the absence of zinc were found to fit reasonably to Herschel-Bulkley model (equation 2) leading to yield stress values (τ_y), fluidification index (n), and the consistency coefficient (K) that are in agreement with most of the literature on these types of gels (Figure 4). When zinc is added to the mixture, the recovered τ_y of the suspending gel (SG) clearly reduces below that of the formulation without zinc for all experimental conditions of this work (Figure 5). τ_y is found to decrease steadily with increasing zinc concentration,

eventually becoming indiscernible at higher concentration (Figure 5). This pattern persists across all examined PAA concentrations, ranging from 0.1 wt% to 0.2 wt%, albeit with a slight variation in the extent of the yield stress (τ_y) reduction (Figure 5). For instance, τ_y is measurable up to a zinc concentration of 10 wt% in 0.1 wt% PAA solutions, whereas for 0.15 wt% PAA, τ_y is measurable up to a zinc concentration of 30 wt%, and it can be measured up to 60 wt% for higher PAA concentrations.

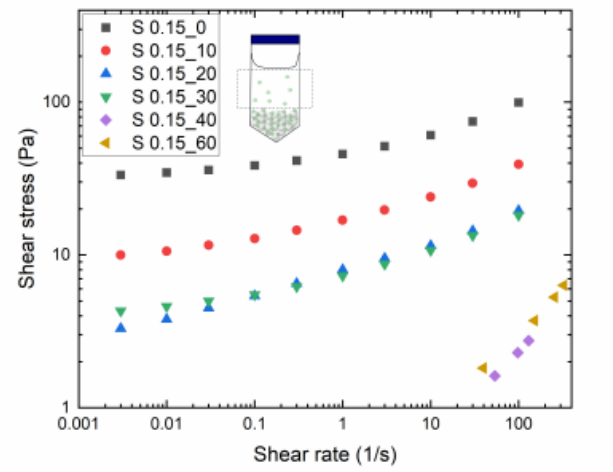

Figure 4. Steady shear stress as a function of shear rate of suspending gels (SG). SG is prepared by mixing PAA at a concentration of 0.15 wt% with zinc at different fractions (0-60 wt%), under agitation, and separated through centrifugation. The legend ($S_{0.15\_zn}$) denotes sample specificity (cf. §2.3). The pH of the sample free of zinc ($S_{0.15\_0}$) is 7, while in the presence of zinc ($S_{0.15}$_zn), the pH is above 10, as reported in figure 3.

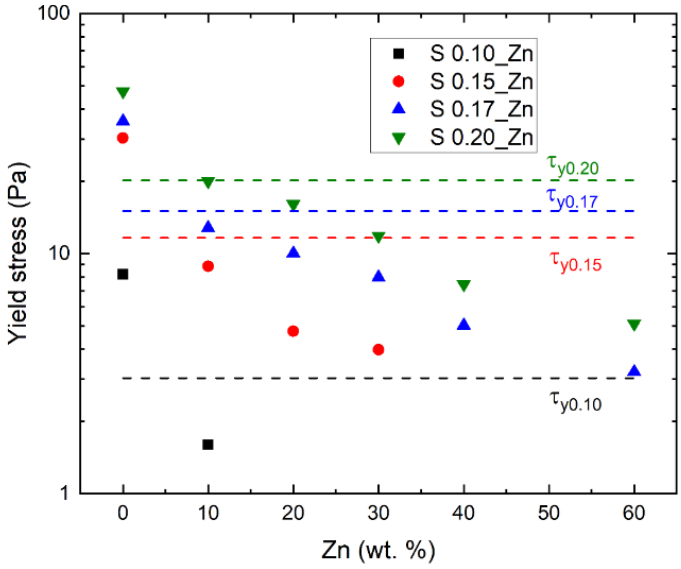

Figure 5: Yield stress of suspending gels (SG) as a function of zinc weight percentage for different initial PAA concentrations (0.1-0.2 wt%). Yield stress values are derived from fitting data to the Herschel-Bulkley model using Figure 4 and supplementary material S2. SGs were prepared by mixing PAA with zinc at varying weight percentages (0 - 60 wt%) under agitation, followed by separation via centrifugation to obtain the supernatant gel, referred to as SG. The legend notation (S_{p_zn}) indicates sample specificity (§2.3). For samples without zinc (S_{p_0}), the pH is 7, whereas samples containing zinc (S_{p_zn}) exhibit a pH above 10, as detailed in figure 3.

Two plausible explanations can be put forward for the observed zinc_induced reduction of viscosity and yield stress:

• The interaction between PAA and zinc can lead to the formation of zinc/PAA complexes, consequently reducing the PAA fraction in the SG. In other words, if less polymer is found in the SG after centrifugation as compared to the initial gel, it suggests that some PAA has adsorbed on zinc particles, which then settles together with zinc during centrifugation.

• As previously mentioned, the redox reaction of Zn generates soluble ionic species, and leads to an increase in the pH from 7 to between 10 and 11 (Figure 3). This increase in ionic strength can result in the screening of repulsive charges in the PAA, causing the PAA microgel to contract and consequently reducing its yield stress (τ_y), as illustrated in Figure 2b. However, it's worth recalling that Figure 2b shows that τ_y decreases by 40 to 50% when increasing the pH from 7 to approximately 10-11, which is significantly lower than the observed zinc-induced reduction of τ_y (Figure 5). For example, the addition of 30 wt% Zn to a 0.15 wt.% PAA gel results in a more than 80% reduction in τ_y, as shown in Figure 5. Therefore, it is probable that the formation of complex zinc/PAA is a major contributor to the yield stress reduction. To gather evidence for this, an alternative method involving fluorescence labeling is employed.

3.4. Characterizing PAA adsorption on zinc using UV-Vis Absorption spectroscopy

To gain further insights into the origin of the Zn-induced reduction of τ_y, UV absorption spectroscopy was employed, using R6G-labeled PAA (PAA-R6G) gel for the preparation of the suspension. Solutions containing 0.1 wt. % PAA-R6G and various concentrations of zinc ranging from 1-20 wt% were kept under agitation for 24 hours, then centrifuged to isolate the SG, which were subsequently analyzed using UV-Vis spectroscopy. The absorption at $\lambda = 529$ nm was measured to determine the molar concentration of R6G in the SG, utilizing the Beer-Lambert's law ($A = \varepsilon \cdot l \cdot c$), with ε set at 92,000 cm^{-1} M^{-1}.

Figure 6 infers a significant reduction in R6G concentration within the SG obtained after centrifugation of the PAA-R6G /zinc suspension with increasing zinc contain. Remarkably, the addition of just 1 wt% zinc led to a 50% decrease in the R6G content in the supernatant, which continue to decrease with further addition of Zn. These findings strongly suggest that PAA-R6G is adsorbed onto the zinc particles, thereby decreasing the amount of PAA-R6G present in the supernatant.

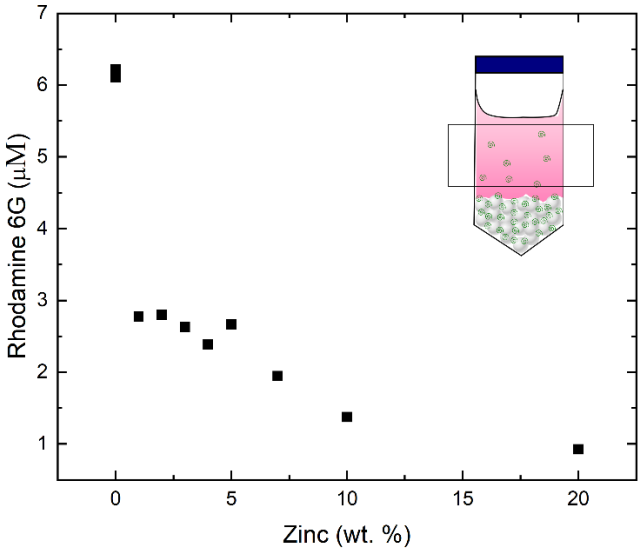

Figure 6. Concentration of Rhodamine 6G, indicative of the remaining PAA-labeled R6G (PAA-R6G) concentration within the SG, is plotted against the Zn fraction in the parent suspension. The SG is formulated by blending 0.1 wt% PAA-labeled R6G (PAA-R6G) with varying fractions of zinc, followed by separation via centrifugation. The concentration of R6G is determined through UV-Vis Absorption spectroscopy.

The rapid decrease in R6G content in the supernatant complicates the quantitative analysis of these results. It suggests that labeling PAA with rhodamine modifies the properties of PAA, thus influencing its adsorption behavior. Consequently, these findings are primarily interpreted as qualitative evidence, reinforcing the initial hypothesis that PAA forms complexes with zinc through adsorption, resulting in a decrease in SG viscosity and yield stress, and thereby impacting its suspending capabilities.

In order to support the above results, the polymer concentration in the supernatant has to be quantified and connected to the SG's viscosity. This was done using inverse rheometry as developed in the following section.

3.5. Quantifying PAA adsorption on zinc through inverse rheometry

To estimate the quantity of PAA adsorbed onto Zn from the yield stress values τ_y presented in Figure 5, a calibration curve is developed by measuring τ_y against PAA concentration, while accounting for the zinc-induced pH increase. Considering that zinc causes the solution's pH to rise to about 11 (figure 3), the τ_y of the PAA gel was measured at this pH across a range of PAA concentrations [PAA] from 0.1 wt% to 0.5 wt%.

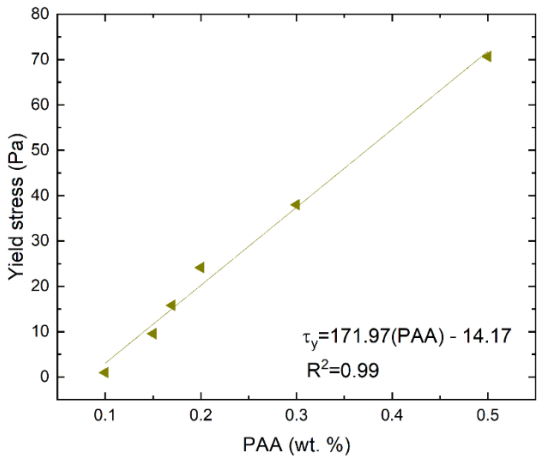

Figure 7. Yield stress of PAA gel as function of PAA concentration at pH = 11.

This resulted in the calibration curve represented in Figure 7 for τ_y vs. [PAA], revealing a linear relationship as depicted by equation 6:

$$\tau_y = 171.97[PAA] - 14.17 \qquad R^2 = 0.99 \qquad (6)$$

Where the yield stress is in Pa and PAA concentration is in wt%.

The PAA concentration within the SG, namely $[PAA]_{supernatant}$, is thus inversely deduced using τ_y values of figure 7 and equation 6. Each determined $[PAA]_{supernatant}$ is then normalized to the PAA concentration in the parent suspension $[PAA]_0$. Thus, the ratio $[PAA]_{supernatant}/[PAA]_0$ will be an indication of the proportion of "free-polymer" remaining in the supernatant as compared to the initial amount $[PAA]_0$. This ratio is plotted against zinc concentration in Figure 8a for each zinc/polymer suspension considered in this study. It is clearly decreasing as the concentration of zinc used in the parent suspensions increases. This decrease is rapid at first and slows down for zinc concentrations above 40 wt% in agreement with several studies (Wright et al. 1998; Eugénie et al. 2014) displaying the decrease of adsorption kinetics as the medium viscosity increases.

This result indicates that for a gel prepared at a given polymer concentration, as more zinc particles are used to prepare suspension, more polymer will be involved in the interactions with zinc, which will automatically result in a lower concentration of free polymer in the supernatant after centrifugation. These findings strongly suggest that the adsorption process is primarily influenced by the quantity of accessible zinc surface area.

The quantity of PAA adsorbed onto zinc $[PAA]_{ads}$ is deduced from the $[PAA]_{supernatant}$ as $[PAA]_{ads} = [PAA]_0 - [PAA]_{supernatant}$. The total available surface area per unit volume is estimated by assuming spherical zinc particles with an average diameter of 76.4 µm for each zinc concentration considered in the parent suspension. Figure 8b quantifies the absorbed PAA polymer as function of contact area of zinc particles and it is observed that $[PAA]_{ads}$ increases steadily with an increase in zinc surface area. This result supports the conclusion that the reduction in the supernatant's yield stress (τ_y) is primarily due to the adsorption of PAA microgel onto the zinc particles.

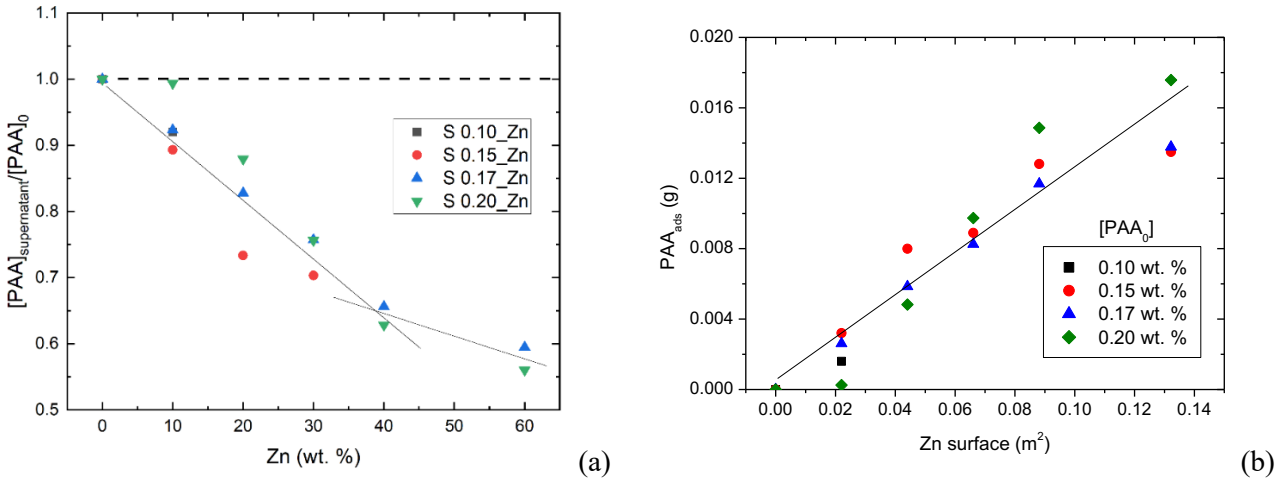

Figure 8. a) Fraction of remaining PAA in supernatant determined by inverse rheometry approach as function of zinc concentration in parent zinc suspension. The ratio $[PAA]_{supernatant}$ is determined from equation 6, using the values of yield stress in figure 5. $[PAA]_0$ is the initial known concentration of the PAA polymer gel (S_{P_0}). Dashed line represents the condition in which no zinc-PAA interactions occur. Calculations are done by considering that the pH of supernatants is 11. Solid line is a visual guide to ease the reading of the figure. b) Amount of PAA that interacted with zinc particles. The straight line represents the rate of PAA interacting with zinc particles, with an average slope value of 0.12 g/m^2 of zinc particles obtained from PAA_0 of 0.10, 0.15, 0.17 and 0.20 wt. %.

The amount of Carbopol® adsorbed onto the Zn surface can be estimated using the linear fit depicted in Figure 8, yielding approximately 0.12 g/m2 ± 0.02 or 2.2 x 10-9 g of PAA per Zn particle. Carbopol® 940 is composed of polydisperse micrometric cross-linked particles that exhibit significant swelling, up to 1000 times, upon neutralization in the absence of added salt (Lee et al. 2011). Consequently, it is plausible that the adsorption of a swollen Carbopol® particle creates an exclusion zone with an area of $\pi/4*D_{PAA}^2$, within which other PAA particles cannot interact with the zinc particles (D_{PAA} representing the diameter of the swollen PAA on the Zn surface). The typical size of the dry PAA particles ranges from 0.2 µm to 6 µm (Jaworski

et al. 2022; Oelschlaeger et al. 2022). For the purpose of this study, assuming a dry PAA size of approximately 2 μm, and considering that the maximum swelling ratio in solution ranges from 1000 times to 500 times for PAA concentrations between 0.1 wt% and 0.2 wt%, we can estimate the extent of the exclusion zone and its dependence on the swelling ratio (Oelschlaeger et al. 2022).

To understand how the adsorption of swollen particles impacts the solution's yield stress, we will explore two extreme scenarios: dry PAA and fully swollen PAA at 0.2 wt%. In the former case, it would require approximately 2.6 x 10^{-8} g of PAA to cover one Zn particle, leading to the majority of the PAA being adsorbed onto the Zn under our experimental conditions. This would result in a substantial reduction in yield stress and hinder the stabilization of the Zn suspension. In the latter scenario, with the maximum swelling ratio being 500 times, only about 5.7 x 10^{-10} g of PAA would be needed to coat one Zn particle, causing only a slight impact on the yield stress and the stabilization of Zn.

In the case of PAA/Zn, as estimated from Figure 8b (2.2 x 10^{-9} g/particle), the adsorbed PAA is swollen 42 times, instead of the maximum 500 times. This outcome can be attributed to the presence of ionic species resulting from the dissolution of Zn (Zhang 1996), which serve to screen the electrostatic repulsive forces within the Carbopol® molecule near the Zn surface, consequently reducing its swelling ratio. Nonetheless, adsorbed swollen particles decrease the adsorption ratio, ultimately enhancing the efficiency of zinc stabilization with Carbopol®.

4. Conclusion

This study explored how zinc microparticles are stabilized using Carbopol® microgels (PAA) in zinc slurry–air redox flow batteries (Zn-RFBs), focusing on their interaction with zinc particles in alkaline conditions. The research showed that PAA is an effective agent for suspending zinc particles, highlighting the need to look beyond just the intrinsic yield stress of the gel. It's essential to consider other interactions within the system, like complexation, adsorption, and zinc redox reactions that release various ionic species. Understanding these interactions is crucial for assessing how they influence the gel's yield stress and its effectiveness in preventing sedimentation.

Results indicated that zinc’s redox reactions produce various ionic species that alter the pH, ionization, and swelling behavior of the PAA gel, thereby reducing its yield stress and impacting zinc stabilization.

The research's key findings suggest that Carbopol® microgel adsorption onto zinc surfaces significantly affects the gel's yield stress and its ability to suspend particles. Techniques like inverse rheometry and UV-Vis spectroscopy highlighted the crucial role of this adsorption in determining the gel's yield stress and its effect on particle suspension.

Overall, these insights deepen our understanding of the physical and chemical interactions within Zn-RFBs and underscore areas for further research to enhance the performance and stability of these battery systems. This knowledge is vital for advancing energy storage technology, especially in applications requiring efficient and reliable battery operation.

Acknowledgements

This project has received funding from the European Union's Horizon 2020 research and innovation program under the Marie Skłodowska-Curie Grant Agreement number 765289.

The Rhéologie et Procédés Laboratory is affiliated with the LabEx Tec 21 (Investissements d'Avenir - Grant agreement no ANR-11-LABX-0030). Additionally, the laboratory is associated with the PolyNat Carnot Institute (Investissements d'Avenir - Grant agreement no ANR-11-CARN-030-01).

References

Atapattu D, Chhabra R, Uhlherr P (1995) Creeping sphere motion in Herschel-Bulkley fluids: flow field and drag. J Non-Newton Fluid Mech 59:245–265

Beija M, Afonso CAM, Martinho JMG (2009) Synthesis and applications of Rhodamine derivatives as fluorescent probes. Chem Soc Rev 38:2410. https://doi.org/10.1039/b901612k

Beris A, Tsamopoulos J, Armstrong R, Brown R (1985) Creeping motion of a sphere through a Bingham plastic. J Fluid Mech 158:219–244

Choi N, del Olmo D, Fischer P, et al (2020) Development of Flow Fields for Zinc Slurry Air Flow Batteries. Batteries 6:15. https://doi.org/10.3390/batteries6010015

Coussot P, Raynaud JS, Bertrand F, et al (2002) Coexistence of Liquid and Solid Phases in Flowing Soft-Glassy Materials. Phys Rev Lett 88:. https://doi.org/10.1103/PhysRevLett.88.218301

Curran S, Hayes R, Afacan A, et al (2002) Properties of carbopol solutions as models for yield-stress fluids. J Food Sci 67:176–180

Dinkgreve M, Fazilati M, Denn MM, Bonn D (2018) Carbopol: From a simple to a thixotropic yield stress fluid. J Rheol 62:773–780. https://doi.org/10.1122/1.5016034

Duduta M, Ho B, Wood VC, et al (2011) Semi-Solid Lithium Rechargeable Flow Battery. Adv Energy Mater 1:511–516. https://doi.org/10.1002/aenm.201100152

Emady H, Caggioni M, Spicer P (2013) Colloidal microstructure effects on particle sedimentation in yield stress fluids. J Rheol 57:1761–1772. https://doi.org/10.1122/1.4824471

Faegh E, Omasta T, Hull M, et al (2018) Understanding the dynamics of primary Zn-MnO2 alkaline battery gassing with operando visualization and pressure cells. J Electrochem Soc 165:A2528

Ferroir T, Huynh H, Chateau X, Coussot P (2004) Motion of a solid object through a pasty (thixotropic) fluid. Phys Fluids 16:594–601

Fu J, Cano ZP, Park MG, et al (2017) Electrically Rechargeable Zinc–Air Batteries: Progress, Challenges, and Perspectives. Adv Mater 29:. https://doi.org/10.1002/adma.201604685

Gutowski IA, Lee D, de Bruyn JR, Frisken BJ (2012) Scaling and mesostructure of Carbopol dispersions. Rheol Acta 51:441–450. https://doi.org/10.1007/s00397-011-0614-6

Haack RA, Gayda S, Himmelsbach RJ, Tetin SY (2017) Unexpected reactivity of the 2′-carboxyl functionality in rhodamine dyes. Tetrahedron Lett 58:1733–1737. https://doi.org/10.1016/j.tetlet.2017.03.054

Han X, Li X, White J, et al (2018) Metal–Air Batteries: From Static to Flow System. Adv Energy Mater 8:. https://doi.org/10.1002/aenm.201801396

Hubbard R, Brown G (1943) Rolling Ball Viscometer. Ind Eng Chem Anal Ed 15:212–218. https://doi.org/10.1021/i560115a018

Jaworski Z, Spychaj T, Story A, Story G (2022) Carbomer microgels as model yield-stress fluids. Rev Chem Eng 38:881–919

Kelessidis VC, Poulakakis E, Chatzistamou V (2011) Use of Carbopol 980 and carboxymethyl cellulose polymers as rheology modifiers of sodium-bentonite water dispersions. Appl Clay Sci 54:63–69. https://doi.org/10.1016/j.clay.2011.07.013

Konarov A, Voronina N, Jo JH, et al (2018) Present and future perspective on electrode materials for rechargeable zinc-ion batteries. ACS Energy Lett 3:2620–2640

Lee D, Gutowski IA, Bailey AE, et al (2011) Investigating the microstructure of a yield-stress fluid by light scattering. Phys Rev E 83:. https://doi.org/10.1103/PhysRevE.83.031401

Lefrançois P, Ibarboure E, Payré B, et al (2015) Insights into C arbopol gel formulations: Microscopy analysis of the microstructure and the influence of polyol additives. J Appl Polym Sci 132:. https://doi.org/10.1002/app.42761

Li S, Deng S, Chen Q, et al (2010) Adsorption of PAA on Surface of CaCO3 Particles and its Effect on Dispersion and Fluid of CACO3 Suspensions. J Polym Eng 30:479–494. https://doi.org/10.1515/POLYENG.2010.30.8.479

Mainar AR, Iruin E, Colmenares LC, et al (2018) An overview of progress in electrolytes for secondary zinc-air batteries and other storage systems based on zinc. J Energy Storage 15:304–328. https://doi.org/10.1016/j.est.2017.12.004

McMahon M, Santucci R, Scully J (2019) Advanced chemical stability diagrams to predict the formation of complex zinc compounds in a chloride environment. RSC Adv 9:19905–19916

Merkak O, Jossic L, Magnin A (2009) Migration and sedimentation of spherical particles in a yield stress fluid flowing in a horizontal cylindrical pipe. AIChE J 55:2515–2525

Merkak O, Jossic L, Magnin A (2006) Spheres and interactions between spheres moving at very low velocities in a yield stress fluid. J Non-Newton Fluid Mech 133:99–108

Milian D, Choi NH, Tsehaye MT, et al (2023) Formulation and characterization of zinc slurries for zinc slurry–Air redox flow battery: A rheological approach. J Power Sources 555:232331

Nelson AZ, Ewoldt RH (2017) Design of yield-stress fluids: a rheology-to-structure inverse problem. Soft Matter 13:7578–7594. https://doi.org/10.1039/C7SM00758B

Oelschlaeger C, Marten J, Péridont F, Willenbacher N (2022) Imaging of the microstructure of Carbopol dispersions and correlation with their macroelasticity: A micro- and macrorheological study. J Rheol 66:749–760. https://doi.org/10.1122/8.0000452

Oppong FK, de Bruyn JR (2011) Mircorheology and jamming in a yield-stress fluid. Rheol Acta 50:317–326. https://doi.org/10.1007/s00397-010-0519-9

Ovarlez G, Bertrand F, Coussot P, Chateau X (2012) Shear-induced sedimentation in yield stress fluids. J Non-Newton Fluid Mech 177:19–28

Ovarlez G, Mahaut F, Deboeuf S, et al (2015) Flows of suspensions of particles in yield stress fluids. J Rheol 59:1449–1486. https://doi.org/10.1122/1.4934363

Parsons R (1964) The kinetics of electrode reactions and the electrode material. Surf Sci 2:418–435

Piau JM (2007) Carbopol gels: Elastoviscoplastic and slippery glasses made of individual swollen sponges. J Non-Newton Fluid Mech 144:1–29. https://doi.org/10.1016/j.jnnfm.2007.02.011

R. Varges P, M. Costa C, S. Fonseca B, et al (2019) Rheological Characterization of Carbopol® Dispersions in Water and in Water/Glycerol Solutions. Fluids 4:3. https://doi.org/10.3390/fluids4010003

Singh SP, Srivastava AK, Steffe JF (1991) Vibration induced settling of a sphere in a Herschel-Bulkley fluid. J Food Eng 13:181–197

Sollich P, Lequeux F, Hébraud P, Cates ME (1997) Rheology of Soft Glassy Materials. Phys Rev Lett 78:2020–2023. https://doi.org/10.1103/PhysRevLett.78.2020

Tabuteau H, Coussot P, de Bruyn JR (2007) Drag force on a sphere in steady motion through a yield-stress fluid. J Rheol 51:125–137

Tran TNT, Clark MP, Chung H, Ivey DG (2020) Effects of Crosslinker Concentration in Poly(Acrylic Acid)-KOH Gel Electrolyte on Performance of Zinc-Air Batteries. Batter Supercaps 3:409–416. https://doi.org/10.1002/batt.201900199

Viota JL, de Vicente J, Durán JDG, Delgado AV (2005) Stabilization of magnetorheological suspensions by polyacrylic acid polymers. J Colloid Interface Sci 284:527–541. https://doi.org/10.1016/j.jcis.2004.10.024

Visco SJ, Nimon VY, Petrov A, et al (2014) Aqueous and nonaqueous lithium-air batteries enabled by water-stable lithium metal electrodes. J Solid State Electrochem. https://doi.org/10.1007/s10008-014-2427-x

Wu G, Lin S, Yang C (2006) Alkaline Zn-air and Al-air cells based on novel solid PVA/PAA polymer electrolyte membranes. J Membr Sci 280:802–808

Wünsch O (1994) Oscillating sedimentation of spheres in viscoplastic fluids. Rheol Acta 33:292–302

Zhang XG (1996) Corrosion and electrochemistry of zinc. Springer Science & Business Media

Zhu YG, Narayanan TM, Tulodziecki M, et al (2020) High-energy and high-power Zn–Ni flow batteries with semi-solid electrodes. Sustain Energy Fuels 4:4076–4085

Figure captions

Figure 1. Apparent sedimentation velocity of zinc particles in gels composed of PAA and attapulgite. PAA concentration was varied between 0.5 wt % and 2 wt %. Attapulgite and zinc concentration were maintained at 10 wt % and 30 wt% respectively. The measurements are determined from results in Milian et al, 2023. These velocities are plotted against the dimensionless yield stress Y, which is derived from the fluid yield stress τ_y using Equation 1.

Figure 2. a) Shear stress as function of shear rate for PAA gel 0.10 wt. % at different pH. b) Yield stress τ_y obtained from Herschel-Bulkley model, as function of pH for different PAA concentrations.

Figure 3. pH variation of SG as a function of Zn weight fraction in parent Zn suspensions. The SG is prepared by mixing PAA at various concentrations (0.1, 0.15, 0.17, and 0.2 wt%) with zinc at different fractions, under agitation, followed by separation through centrifugation. The supernatant, designated as the SG, is then subjected to pH measurement. The legend (Sp_zn) denotes sample specificity, where "p" represents the fraction of the initial PAA concentration.

Figure 4. Steady shear stress as a function of shear rate of suspending gels (SG). SG is prepared by mixing PAA at a concentration of 0.15 wt% with zinc at different fractions (0-60 wt%), under agitation, and separated through centrifugation. The legend (S0.15_zn) denotes sample specificity (cf. §2.3). The pH of the sample free of zinc (S0.15_0) is 7, while in the presence of zinc (S0.15_zn), the pH is above 10, as reported in figure 3.

Figure 5: Yield stress of suspending gels (SG) as a function of zinc weight percentage for different initial PAA concentrations (0.1-0.2 wt%). Yield stress values are derived from fitting data to the Herschel-Bulkley model using Figure 4 and supplementary material S2. SGs were prepared by mixing PAA with zinc at varying weight percentages (0 - 60 wt%) under agitation, followed by separation via centrifugation to obtain the supernatant gel, referred to as SG. The legend notation (Sp_zn) indicates sample specificity (§2.3). For samples without zinc (Sp_0), the pH is 7, whereas samples containing zinc (Sp_zn) exhibit a pH above 10, as detailed in figure 3.

Figure 6. Concentration of Rhodamine 6G, indicative of the remaining PAA-labeled R6G (PAA-R6G) concentration within the SG, is plotted against the Zn fraction in the parent suspension. The SG is formulated by blending 0.1 wt% PAA-labeled R6G (PAA-R6G) with varying fractions of zinc, followed by separation via centrifugation. The concentration of R6G is determined through UV-Vis Absorption spectroscopy.

Figure 7. Yield stress of PAA gel as function of PAA concentration at pH = 11

Figure 8. a) Fraction of remaining PAA in supernatant determined by inverse rheometry approach as function of zinc concentration in parent zinc suspension. The ratio [PAA]supernatant is determined from equation 6, using the values of yield stress in figure 5. [PAA]0 is the initial known concentration of the PAA polymer gel (SP_0). Dashed line represents the condition in which no zinc-PAA interactions occur. Calculations are done by considering that the pH of supernatants is 11. Solid line is a visual guide to ease the reading of the figure. b) Amount of PAA that interacted with zinc particles. The straight line represents the rate of PAA interacting with zinc particles, with an average slope value of 0.12 g/m^2 of zinc particles obtained from PAA_0 of 0.10, 0.15, 0.17 and 0.20 wt. %.

Supporting Information

S1. Supernatant SEM picture.

A SEM picture from a dried PAA supernatant (after being in contact with zinc particles), is depicted in figure S1. It is observed that residual zinc particles are not present in the dried supernatant (D_{50}=76.4 µm). The crystals observed on the picture on the right are dissolved zinc species that precipitate at pH 11, like ZnO (Mainar et al. 2018).

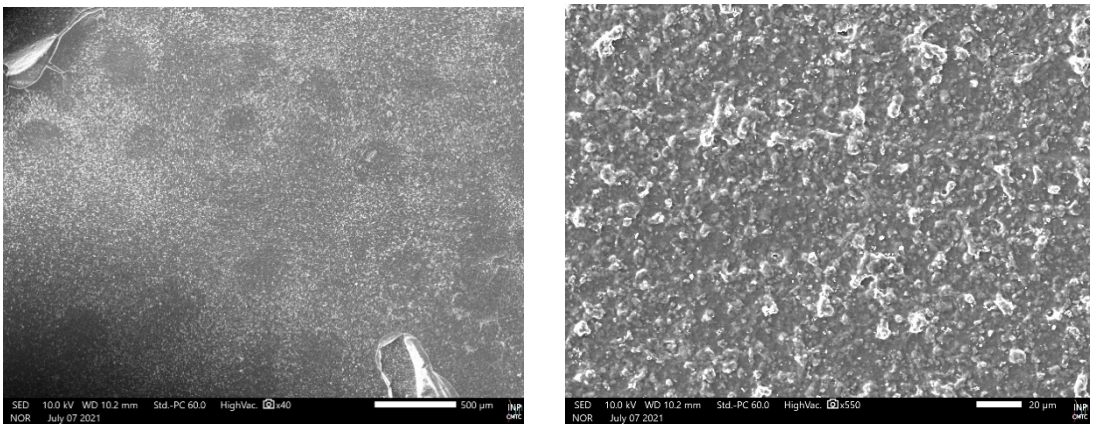

Figure S1. SEM picture of dried supernatant $S_{0.15\_20}$. a) x40 Scalebar 500 µm. b) x550, scalebar 20 µm.

S2. Steady state flow curves from supernatants

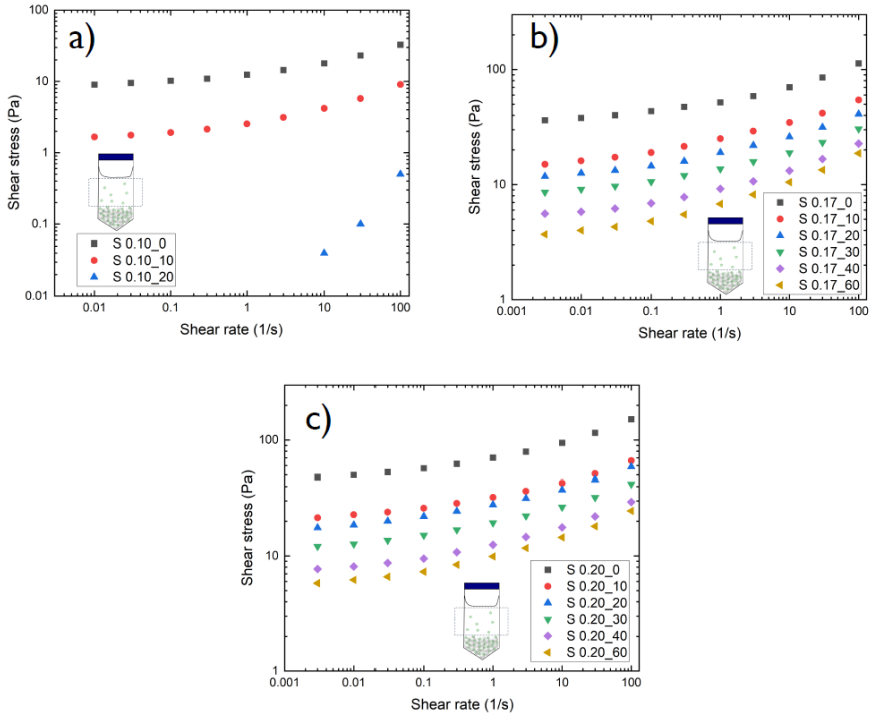

Figure S2. Supernatants steady state rheometry at pH 11. a) $S_{0.10\_Zn}$, b) $S_{0.17\_Zn}$ and c) $S_{0.20\_Zn}$ shear stress as function of shear rate obtained from centrifugation of zinc parent suspensions.

Supernatants obtained from suspensions prepared from PAA gel 0.10 wt. % are observed in figure S2a. It is observed that original gel $S_{0.10\_0}$ has a viscoplastic behavior denoted by the yield stress. In fact, as zinc particle concentration in parent suspension is increased, shear stress values decrease. Moreover, as equivalently observed for $S_{0.15\_Zn}$ in figure 5, it is observed that at a zinc concentration of 20 wt. %, viscoplastic behavior has already vanished.

For supernatants prepared from PAA gel 0.17 wt. % and 0.20 wt. %, in figure S2b and S2c, respectively. It is observed that shear stress decreases as zinc concentration used to prepare zinc suspensions increase. It is remarked that for these initial PAA concentrations, viscoplastic behavior is observed whatever the zinc concentration considered in the studied range from 10 to 60 wt. %.